

Biological Activity of Poly(1,3-propanediol citrate) Films and Nonwovens: Mechanical, Thermal, Antimicrobial, and Cytotoxicity Studies

Aleksandra Bandzerewicz, Kamil Wierzchowski, Jolanta Mierzejewska, Piotr Denis, Tomasz Gołofit, Patrycja Szymczyk-Ziółkowska, Maciej Pilarek, and Agnieszka Gadomska-Gajadhur*

Polymers are of great interest for medical and cosmeceutical applications. The current trend is to combine materials of natural and synthetic origin in order to obtain products with appropriate mechanical strength and good biocompatibility, additionally biodegradable and bioresorbable. Citric acid, being an important metabolite, is an interesting substance for the synthesis of materials for biomedical applications. Due to the high functionality of the molecule, it is commonly used in biomaterials chemistry as a crosslinking agent. Among citric acid-based biopolyesters, poly(1,8-octanediol citrate) is the best known. It shows application potential in soft tissue engineering. This work focuses on a much less studied polyester, poly(1,3-propanediol citrate). Porous and non-porous materials based on the synthesized polyesters are prepared and characterized, including mechanical, thermal, and surface properties, morphology, and degradation. The main focus is on assessing the biocompatibility and antimicrobial properties of the materials.

1. Introduction

The intensive development of tissue engineering offers new possibilities for reconstructing damaged tissues. Tissue engineering aims to combine biological material (cells) and a synthetic scaffold that temporarily supports the growing tissue. Such scaffolds are mainly made of biodegradable polymers, for example, polyesters.^[1] New biomaterials with better biocompatibility and application properties are being researched. Both natural and synthetic biopolymers are used. Materials of natural origin have the advantage of being non-toxic and minimizing the host's immune response. However, the application requirements are growing, which leads to an increasing emphasis on the ability to functionalize the material and an ease of processing into a product with tailorable properties. As a result, synthetic polymers

are becoming widely relevant. The solution to their biocompatibility problem is using substrates naturally present in the body. These include citric acid, an intermediate in the Krebs cycle that occurs in the metabolism of all aerobic organisms. Besides, biodegradability is considered a crucial and desired property in many applications as it contributes to sustainability by reducing waste. Polymers that are degradable to substances present in the body are called bioresorbable. The degradation products are subsequently included in metabolic pathways, excluding the necessity of removing the biomaterial device once its function has been fulfilled.^[2,3] For some applications, additional properties of biopolymers are in demand, for example, antimicrobial activity. Considering the severity of the problems caused by microbial contamination, such qualities are mostly desired in food packaging and biomedical devices.^[4]

In the natural environment, polyesters are hydrolyzed to acidic oligomers and monomers. Hence, the degradation process might result in a significant drop in the local pH leading to an inhibited growth of microorganisms as they typically prefer a pH greater than 4.^[5] Many environmental factors affect microbial metabolic activities; however, acidity is critical.^[6] First, because of the pH-dependency of structure and function of biological macromolecules (especially proteins). Second, because of protons

A. Bandzerewicz, J. Mierzejewska, T. Gołofit, A. Gadomska-Gajadhur
 Faculty of Chemistry
 Warsaw University of Technology
 3 Noakowskiego Street, Warsaw 00-664, Poland
 E-mail: agadomska@ch.pw.edu.pl
 K. Wierzchowski, M. Pilarek
 Faculty of Chemical and Process Engineering
 Warsaw University of Technology
 Waryńskiego 1 Street, Warsaw 00-645, Poland
 P. Denis
 Laboratory of Polymers and Biomaterials
 Institute of Fundamental Technological Research Polish Academy of Sciences
 Pawińskiego 5B Street, Warsaw 02-106, Poland
 P. Szymczyk-Ziółkowska
 Centre for Advanced Manufacturing Technologies—Fraunhofer Project Center
 Faculty of Mechanical Engineering
 Wrocław University of Science and Technology
 Lukasiewicza 5, Wrocław 50-371, Poland

 The ORCID identification number(s) for the author(s) of this article can be found under <https://doi.org/10.1002/marc.202300452>

DOI: 10.1002/marc.202300452

concentration affecting the kinetics of chemical reactions. The final reason is the impact of pH changes on the energetic metabolism (electrochemical potential for ATP synthesis).^[7] Every microbe exhibits optimal growth pH, which is the pH of its maximum growth rate. In natural environments, a one-unit pH change can lower the metabolic activity of microbial communities by up to 50%.^[8,9] However, a simple pH drop is not sufficient for the inhibition of the microorganisms to occur as they can form a resilient colony if there is a substantial time discrepancy between the microbial growth and the degradation-driven environment acidifying. To overcome the problematic mismatch, a fast-degrading polymer is needed. This, in turn, entails the increased risk of inflammation of the surrounding tissues and rapid loss of the required mechanical properties of the material.^[5,10]

At present, there are several types of biodegradable polyesters on the market. Among them, poly-L-lactide (PLA) has been attracting much attention for some time now because it is readily available and relatively inexpensive. Depending on the physicochemical and mechanical properties, PLA has found applicability in packaging and a wide range of biomedical uses, for example, bone fixation screws, suture threads, and drug delivery systems.^[11,12] Thermal stability and degradation rate of PLA are determined by crystalline content and molecular weight, which affect its processability (due to brittleness).^[13,14] To address the limitations, PLA has been blended with various polymers.^[15–19] Other promising materials in medical and packaging sectors include polycaprolactone, polyhydroxyalkanoates, poly(glycolic acid), and poly(glycerol sebacate).^[14,20–24] Blending biodegradable polymers with natural biopolymers synthesized from renewable resources (e.g., starch) expands their industrial applications by minimizing cost.^[24]

The potential of PLA for use in antibacterial packaging has been investigated. However, in those studies, antimicrobial activity is achieved by incorporating active agents, nanoparticles, or essential oils into PLA, not due to the properties of the polymer itself.^[25–29] PLA film then acts as an active release system, and the release kinetics can be tuned by modifying the physical properties and crystallinity of the polymer film resulting from different processing techniques.^[30] Studies on such matrixes based on biodegradable polyesters also include poly(3-hydroxybutyrate) and poly(butylene succinate) (PBS). Still, the antimicrobial activity is obtained via specific additives and polymer backbone functionalization. The results imply that the aforementioned materials might exhibit too slow a degradation rate to act as antimicrobial agents on their own.^[31–33] Having said that, citric acid has recently emerged as an interesting monomer for biomaterial synthesis. Simultaneously, it has been reported as an antimicrobial molecule, although the knowledge of the action mechanism remains limited. The uncharged molecule is believed to penetrate the microbial membrane and dissociate once inside the cytoplasm, causing acidification and, subsequently, structural damage to the cell. Negatively charged citric acid species are thought to destabilize the outer membrane or sequester metals essential for the bacteria's growth from its environment.^[34] Given the positive results of cytotoxicity testing of citric acid-based polyesters and various poly(glycerol dicarboxylates), the potential of such materials as antimicrobial scaffolds for cell culture is deemed worthwhile studying.^[35–38] With the aim to contribute to increas-

ing the range of potential biomaterials, it was decided to test the cytotoxicity and antimicrobial activity of poly(1,3-propanediol citrate), which has not been reported yet.

2. Experimental Section

2.1. Prepolymer Synthesis Procedure

Commercially available 1,3-propanediol (ChemSolute, >= 99,7%), anhydrous citric acid (Acros Organics, >= 99,5%), and *p*-toluenesulfonic acid monohydrate (Sigma-Aldrich, >= 98,5%) were used without prior preparation. The synthesis of poly(1,3-propanediol citrate) (PDCit) was carried out in the MultiMax Mettler Toledo reactor systems, in Hastelloy reactors (50 mL) equipped with mechanical stirrers, temperature sensors, and Dean–Stark apparatuses. Anhydrous citric acid, 1,3-propanediol, and *p*-toluenesulfonic monohydrate were weighed into the reactor in each trial. The molar ratio of COOH:OH functional groups was 2:1, 1:1, and 1:2. 1% w/w of the catalyst was used in relation to the mass of citric acid. The OH group in the acid molecule was not considered in the calculations. The reaction mixture was heated for 10 min to reach 130 °C. Then the temperature was held constant for 50 min.

2.2. Polymer Film Preparation

The prepolymer mass was heated to about 50 °C and poured into a flat, rectangular PTFE form. The form with the prepolymer was placed in a laboratory oven at 130 °C for 24 h.

2.3. Electrospinning

PLA (Purasorb PL49, Corbion) was used to prepare PLA/PDCit solutions. 1,1,1,3,3,3-Hexafluoro-2-propanol (Iris Biotech) was used as a solvent, and the weight content of polymers was 5% total. The polymer mass ratio varied from 1:3 PLA/PDCit, through 1:1 PLA/PDCit to 3:1 PLA/PDCit. Solutions were stirred for 48 h. The electrospinning process was carried out under the following conditions: applied voltage of 10.5–12.0 kV, solution dosing rate of 1.5 mL h⁻¹, and distance between the needle tip and the surface of the collector 14 cm. A rotational collector with a low linear speed (1 m s⁻¹) was used.

2.4. Scanning Electron Microscopy

Samples were coated with a 7–9 nm thick gold layer in a K550X Sputter Coater. SEM images were taken using a Hitachi TM1000 microscope.

2.5. Gel Content

Rectangular-shaped pieces of ≈6 × 10 mm were cut from the polymer films, three from each test material. The samples were weighed, placed in plastic test tubes with caps, and then submerged in 1 mL of distilled water. The tubes were placed on

a Heidolph reciprocating shaker equipped with a thermostatic chamber for 24 h. A constant temperature of 25 °C and a speed of 150 rpm were maintained throughout the test. Wet samples were dried and weighed again. Drying was carried out at room temperature under 20 mbar for 96 h. Gel content, that is, the degree of the material crosslinking, was calculated according to the formula

$$\text{gel content} = \frac{\text{dry sample mass after testing}}{\text{sample mass before testing}} \times 100\% \quad (1)$$

Results from three trials were averaged. The value of standard deviation was calculated.

2.6. Wettability (Contact Angle) Surface Free Energy Determination

Two liquids were used: distilled water and diiodomethane. Samples were placed on the measuring device, and tiny drops of liquid were placed onto the test surfaces. The droplet's shape was recorded using the Digital Camera Industrial Digital Camera UC-MOS01300KPA with Fixed Microscope Adapter FMA037. The measurements were carried out using the TouPView software. Five samples were taken for each tested material, and the results were averaged.

Based on the results of the contact angle measurements, the surface free energy (SFE) of the materials was determined by applying the Owens–Wendt method.

2.7. Mechanical Tests

The nonwovens were tested on the Mecmesin Multitest-I (Mecmesin Ltd, West Sussex, UK) test frame using a 1 kN load cell. Samples were gripped and elongated at a 10 mm min⁻¹ speed until failure occurred. Young's modulus, maximum tensile force at break, and elongation at break were calculated from the obtained strain–elongation curves. For each sample, three individual measurements were made. The value of standard deviation was calculated.

2.8. Differential Scanning Calorimetry

DSC measurements were taken using TA Instruments Q2000 flow calorimeter. The test was conducted at –50–250 °C with a constant temperature increment of 10 °C min⁻¹. The system was heated, cooled, and heated again.

From the second heating curve, the enthalpy of fusion was determined and on its basis the degree of crystallinity of the samples was calculated according to the formula

$$\% \text{ crystallinity} = \frac{\Delta H_f}{\Delta H_f^0} \times 100\% \quad (2)$$

where ΔH_f —enthalpy of fusion of the sample, J g⁻¹ and ΔH_f^0 —enthalpy of fusion of 100% crystalline PLLA, 93,6 J g⁻¹.^[39]

Results from three trials were averaged. The value of standard deviation was calculated.

2.9. Film Degradation Testing

Rectangular-shaped pieces of $\approx 8 \times 13$ mm were cut from the polymer films, three from each test material. The samples were weighed, placed in plastic test tubes with caps, and then submerged in 5 mL of PBS solution. The tubes were placed on a Heidolph reciprocating shaker equipped with a thermostatic chamber. A constant temperature of 37 °C and a speed of 150 rpm were maintained throughout the test. Wet samples were weighed immediately after removal from the test tube, then dried and weighed again. Drying was carried out at room temperature under 20 mbar for 96 h. The weight loss after 5 and 24 h and after 3, 7, 30, and 60 days was determined according to the formula

$$\text{remaining mass} = \frac{\text{dry sample mass after testing}}{\text{sample mass before testing}} \times 100\% \quad (3)$$

It was also determined how much liquid the material could hold within.

$$\text{mass absorbability} = \frac{\text{wet sample mass after testing}}{\text{dry sample mass after testing}} \times 100\% \quad (4)$$

Results from three trials were averaged. The value of standard deviation was calculated.

2.10. Radiation Sterilization

Cytotoxicity and antimicrobial activity studies were preceded by radiation sterilization of the materials. An electron accelerator ELEKTRONIKA 10/10 was used, and the electron energy was 9.1 MeV. A radiation dose of 15.0 kGy was applied.

2.11. Cytotoxicity Testing

The referential continuous cell line of L929 mouse fibroblasts (ATCC), as model cells of connective tissue exhibit anchorage-dependency, was used. Two Dulbecco's modified Eagle medium (DMEM) media varying in glucose concentration were independently used in the studies: 1 and 4.5 g L⁻¹. Both media were supplemented with 10% v/v inactivated fetal bovine serum and 1% v/v Pen–Strep. All culture media were supplied by Gibco, and they were all certified as approved for cell cultures.

2.11.1. Maintaining L929 Cells

The used culture medium was aseptically pipetted out from culture flasks containing L929 cells. The remaining cell monolayer was rinsed twice with sterile Dulbecco's phosphate buffered saline (DPBS) without Ca²⁺ and Mg²⁺ to remove calcium and magnesium ions from the cells' surface entirely. 3 mL of sterile 0.05% trypsin-EDTA was poured into each flask. The flasks were subsequently incubated for 5 min at 37 °C. Microscopic observation of the cells was performed to assess cell detachment. Suspension of detached cells was transferred to a sterile Falcon-type centrifuge tube, 10 mL of fresh culture medium was added, and

the tube was centrifuged at 4500 rpm for 5 min. The supernatant was aseptically removed, and the cells were suspended in 10 mL fresh culture medium. Cells were counted in a hemocytometer, passaged into new culture flasks, and continuously incubated at 37 °C in 5% CO₂-enriched air atmosphere.

2.11.2. XTT Cytotoxicity Test

Discs of 1.5 cm diameter were cut from the nonwovens and films and placed in 24-well plates, four discs a well for nonwovens and one disc a well for films. The plates were vacuum-packed and sterilized. 1.3 mL or 2.0 mL of culture medium was poured into each well containing the nonwoven and film discs, respectively. The plates were incubated at 37 °C for 24 h.

A cell suspension of 10⁵ cells mL⁻¹ was placed in a 96-well plate, 100 µL per well. The outer wells of the plate were flooded with DPBS to prevent evaporation of the culture medium. The plates were incubated at 37 °C for 24 h. The medium was removed, and the extracts were added, 100 µL per well. Some wells were flooded with fresh medium (negative control) or 0.1% solution of the Triton X-100 in DMEM (positive control). The plate was subsequently incubated at 37 °C for 24 h in 5% CO₂-enriched air atmosphere.

After the incubation, the used culture medium was removed, and the cells were washed twice with 100 µL of DPBS. XTT reagent (CyQUANT XTT Cell Viability Assay, ThermoFisher Scientific) solution in culture medium (33% v/v) was added, 150 µL per well. The 96-well plate was placed in an incubator (37 °C) for 4 h. The absorbance was automatically measured in the multiwell plate reader for 450 and 630 nm (reference wavelength). The test was performed simultaneously in six wells of the 96-well plate for each type of material. Results were compared to the negative control, which was assumed as 100% of the metabolic activity of cells.

2.12. The Proliferation of L929 Cells on the Nonwovens

Discs of 1.5 cm diameter were cut from the nonwovens and films and placed in 24-well plates, one disc a well. The plates were vacuum-packed and sterilized. 1.5 mL of inoculum (10⁵ cells mL⁻¹) was poured into each well. The plates were transferred to an incubator (37 °C, 5% CO₂).

L929 cell cultures were carried out for 8 days without medium exchange. The samples were harvested every 48 h. The following tests or measurements were carried out: cell density and viability assessment (trypan blue dye), metabolic activity (Presto Blue assay), and lactate dehydrogenase activity (LDH assay). SEM and confocal microscopy were also used to visualize the morphology of L929 cells. Zero day analyses were performed after 3 h of incubation.

2.13. Assessment of Properties of Cell Culture

2.13.1. Measurement of Cell Density and Viability

L929 cells were detached from the surface of the nonwovens as per the typical trypsinization procedure. The culture medium was

aseptically pipetted-out from each well. The cells that remained on the nonwovens were rinsed twice with sterile DPBS without Ca²⁺, Mg²⁺ buffer. Then, 0.5 mL of sterile 0.05% trypsin-EDTA was poured into each well. The plates were incubated at 37 °C for 15 min, and the contents were gently mixed with a pipette tip to facilitate the detachment of the cells from the material's surface. 0.5 mL of fresh DMEM medium was added to inhibit trypsin and preserve suspended cells from trypsin-based digestion. Cell density and viability were determined by counting cells stained with 0.4% trypan blue aqueous solution (Thermo Fischer Scientific, US) using a Bürker-Türk hemocytometer (Brand, DE) and an Eclipse TS100 inverted microscope (Nikon) to ensure the replicability of the counting. The counting of the total number of cells and the number of dead cells was repeated five times.

2.13.2. Metabolic Activity Assessment

Metabolic activity has been estimated based on the resazurin-based PrestoBlue assay results (Presto-Blue, Thermo Fischer Scientific, US). 111 µL of PrestoBlue reagent was added to 1.0 mL of L929 cells culture or pure culture medium without cells (reference samples). All samples were incubated at 37 °C for 2 h. Then, absorbance was measured using a GENESYS 20 UV-vis spectrophotometer (Thermo Fisher Scientific, US) at 570 and 600 nm (reference wavelength). Metabolic activity was calculated according to the formula

$$\text{metabolic activity} = 37.04 \times (A_{570} - A_{570\text{REF}}) - (A_{600} - A_{600\text{REF}}) \left[\mu \text{ dm}^{-3} \right] \quad (5)$$

where A_{570} —the absorbance of the test sample at 570 nm, $A_{570\text{REF}}$ —the absorbance of the reference sample at 570 nm, A_{600} —the absorbance of the test sample at 600 nm, and $A_{600\text{REF}}$ —the absorbance of the reference sample at 600 nm,

Results from three trials were averaged. The value of standard deviation was calculated.

2.13.3. LDH Activity Measurement

LDH activity was determined according to the procedure of enzyme-based BioMaxima-LDH assay (BioMaxima, PL). Biomaxima-LDH reagent was prepared by mixing R1 and R2 reagents in a 4:1 volume ratio before use. The reagent was then poured into the standard disposable spectrophotometric cuvettes, 1.0 mL per cuvette. Then, 20 µL of culture medium samples filtered through syringe filters ($\phi = 0.2 \mu\text{m}$) were added and thoroughly mixed. Absorbance measurement was performed at 340 nm in 1 min intervals (from 0 to 3 min) using a GENESYS 20 UV-vis spectrophotometer (Thermo Fisher Scientific, US). The values of LDH activity were calculated based on the following formula

$$\text{LDH activity} = 267.2 \cdot \Delta A \left[\mu \text{ dm}^{-3} \right] \quad (6)$$

where ΔA —the absorbance change per minute.

Results from three trials were averaged. The value of standard deviation was calculated.

2.13.4. Morphology and Cell Culture Visualization

After 0, 2, 4, 6, and 8 days of culture, nonwoven discs with cells were transferred to new 24-well plates and rinsed twice with 1 mL sterile DPBS without Ca²⁺, Mg²⁺ buffer. Next, the materials were soaked in the following solutions: 1 mL of 4% w/v aqueous paraformaldehyde solution (Sigma-Aldrich), 1 mL of 0.2% v/v aqueous Triton X-100 solution (Sigma-Aldrich), 200 µL of 165 nm Alexa Fluor 488 Phalloidin (Thermo Fisher Scientific) in DPBS solution, and 100 µL of 300 nm DAPI (Thermo Fisher Scientific) in DPBS solution. After each step, the materials were rinsed twice with 1 mL sterile DPBS without Ca²⁺, Mg²⁺ buffer. Samples were visualized by an LSM 880 confocal laser scanning microscope (Carl Zeiss AG, Jena, DE).

2.14. Antimicrobial Activity Studies

The antimicrobial activity of PDCit films (molar ratio of COOH:OH functional groups 2:1, 1:1, and 1:2) was tested against gram-positive and gram-negative bacteria and yeast. Tests were conducted in a liquid and on a solid medium. The following microorganisms were used: *Staphylococcus aureus* (*S. aureus*) ATCC 6538, *Escherichia coli* (*E. coli*) ATCC 8739, and *Candida albicans* (*C. albicans*) ATCC 10 231.

2.14.1. Preparation of Cultures of Bacteria and Yeast

A sterile loop of material from a single colony of bacterium or yeast was used to inoculate 10 mL of liquid MHB (for bacteria) or Sabouraud (for yeast) medium in a 100 mL Erlenmeyer flask. The cultures were incubated overnight (about 20 h) at 37 °C with constant shaking (220 rpm) using a Benchtop shaker LabCompanion SI-600R (Jeio Tech, Daejeon, South Korea). Subsequently, the overnight cultures were diluted in fresh medium (MHB or Sabouraud) to obtain a 10⁵ cfu mL⁻¹ suspension of microorganisms.

2.14.2. Tests in a Liquid Medium

Discs of 1.5 cm diameter cut from sterile films, nine from each test material, were placed in 100 mL Erlenmeyer flasks. 5 mL of the previously prepared suspension of 10⁵ cfu mL⁻¹ was added to each flask (three flasks of the same microorganism type for every material). The flasks were placed in the incubator shaker (220 rpm) at 37 °C for 24 h. After 24 h of incubation, the optical density (OD) of the cultures was measured using the spectrophotometric method at the wavelength 600 nm. The results were compared to the OD of the control flasks without materials. Antimicrobial activity was calculated according to the formula

$$\text{antimicrobial activity} = \frac{\text{OD}}{\text{OD}_{\text{control}}} \times 100\% \quad (7)$$

where; OD—optical density of a culture of microorganisms with the addition of the polymer film; OD_{control}—optical density of a culture of microorganisms without the addition of the polymer film.

Results from three trials were averaged. The value of standard deviation was calculated.

Table 1. The gel content of films with different COOH:OH molar ratios.

	COOH:OH molar ratio of poly(1,3-propanediol citrate)		
	1:2	1:1	2:1
gel content [%]	95 ± 2	100 ± 1	84 ± 3

2.14.3. Tests on a Solid Medium

Freshly prepared media (MHA for bacteria and Sabouraud dextrose agar for yeast) were poured into petri dishes and allowed to solidify. Briefly, 100 µL of 10⁸ cfu mL⁻¹ cell suspension was distributed evenly on a suitable medium and allowed to dry. Discs of 1.7 cm diameter cut from sterile films were placed on the petri dishes. The samples were incubated at 37 °C for 24 h. After incubation, sample activity was determined by measuring the diameter of inhibition of the growth zone. Results from three trials were averaged. The value of standard deviation was calculated.

3. Results and Discussion

3.1. Polymer Films

3.1.1. Gel Content

The gel content of the polymer films with different molar ratios of COOH:OH functional groups (2:1, 1:1, and 1:2) was determined, that is, the content of the insoluble phase (crosslinked, gelled) (Table 1).

The highest content of the water-insoluble phase was observed in material with an equimolar ratio of functional groups. It is to be expected as crosslinking should be most readily achieved in this case. Noticeably lower gel content for the film with excess carboxyl groups can be associated with acidification of the environment and faster degradation of the material. The lower crosslinking density in the case of a non-equimolar ratio of COOH:OH results from the presence of free side groups, increasing the interchain distance in the network structure. As a consequence, the permeation of the medium into the material is easier, driving the degradation further.

3.1.2. Wettability and Surface Free Energy

The contact angle values of the surfaces of poly(1,3-propanediol citrate) films were determined (Figure 1). It was observed that the surfaces of all the films tested showed wettability for both liquids, that is, a droplet was formed for each measurement, and the contact angle was less than 90°. No liquid was found to spread over the surface or penetrate the material during the several seconds of measurement duration.

The water contact angle falls within (57.6 ± 4.7)–(71.4 ± 4.0)°. In all three cases, this is a larger value than the diiodomethane contact angle (from (42.4 ± 4.5) to (48.2 ± 3.5)°). This means the non-polar liquid wets the film surfaces more easily than the polar liquid. The film characterized by excess carboxyl groups is the most difficult to wet by water. This indicates that hydroxyl groups hydrophilize the surface more than carboxyl groups. The use of

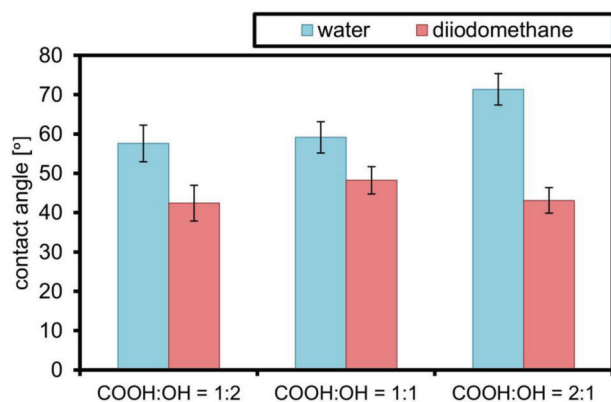


Figure 1. Water and diiodomethane contact angle values of films with different COOH:OH molar ratios.

citric acid helps to increase the hydrophilicity of the film surface compared to similar polyesters based on acids with a longer carbon chain in the molecule, such as poly(glycerol sebacate).^[40]

The polymer chains are arranged in a specific way in the films. There are no free surface functional groups, which mainly determine the hydrophilicity. The wettability of the film surface may be influenced by the material used to make the forms for crosslinking the prepolymer. As a hydrophobic material, PTFE might have induced an arrangement of the polyester chains that ensured minimal contact between the polar groups and the form. The effect of PTFE can also be seen in the fact that hydrophilicity is apparently not affected by the amount of unreacted functional groups remaining after the reaction. The material containing excess carboxyl groups has the least hydrophilic surface despite the theoretically lowest degree of esterification (lowest gel content). This conclusion is worth considering for further studies, for example, by determining the contact angle of films obtained from the same prepolymer but in forms made of different materials.

When analyzing the films for potential use as implantable materials, it ought to be noted that an excess of hydroxyl groups should favor the adsorption of proteins on the surface. First, this is indicated by the SFE values (Figure 2). The higher the SFE value of the film, the stronger the interaction with other materials will be. Besides, proteins that promote cell adhesion are more likely to be absorbed on hydrophilic surfaces.^[41] Materials with COOH:OH molar ratios of 1:2 and 1:1 show higher hydrophilic-

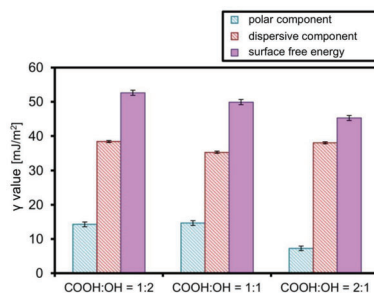


Figure 2. Surface free energy and its components of films with different COOH:OH molar ratios.

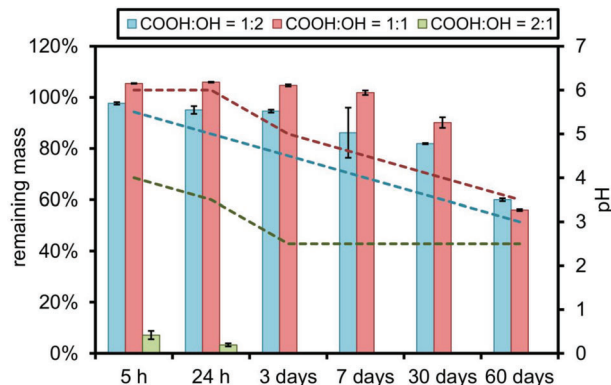


Figure 3. Degradation of films with different COOH:OH molar ratios—changes in the remaining mass of the films (bars on the graph) and pH value of buffer (dashed lines) over time.

ity than the third film, as evidenced by the higher value of the polar component.

3.1.3. Degradation

The degradation time of polymer films in PBS solution at 37 °C was investigated. The test conditions were designed to imitate human body temperature. Weight loss after 5 and 24 h and 3, 7, 30, and 60 days were determined. The initial pH value of the PBS solution was 7.4.

Degradation of the film samples with the highest acid content (COOH:OH = 2:1) occurred almost immediately. Already after 5 h, the weight loss was about 90%. After 24 h, the residual samples had disintegrated into small pieces, which caused problems when weighing. After 3 days, no solid fragments of the samples were found in the tubes. Compared to the other samples, such a rapid weight loss indicates degradation autocatalyzed by free acid groups. The high concentration of H⁺ cations in the medium accelerates the hydrolysis of the ester bonds, causes the release of carboxyl groups, and drives a rapid drop in pH value. The effect illustrated in Figure 3 is, therefore, a synergy between the impact of the medium (water-induced hydrolysis of the ester bonds) and

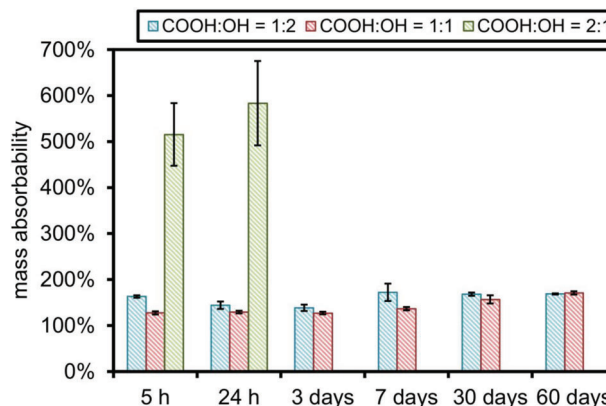
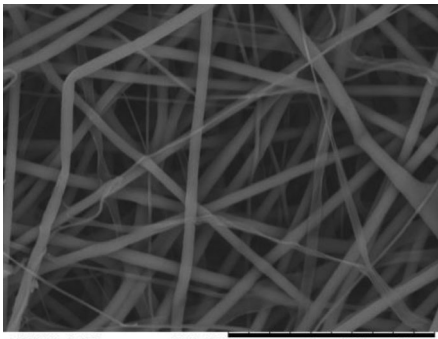
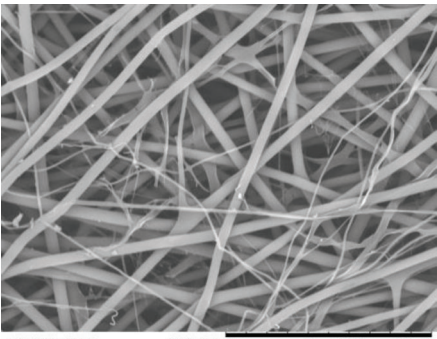
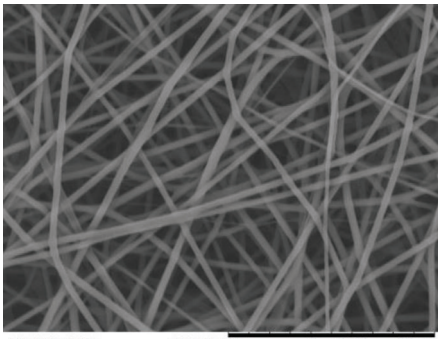
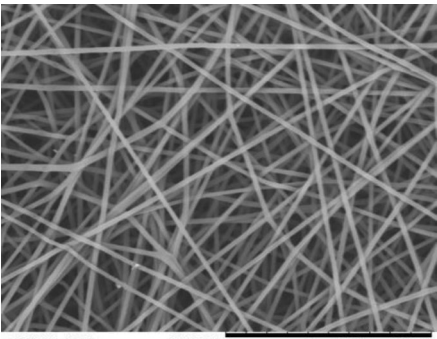
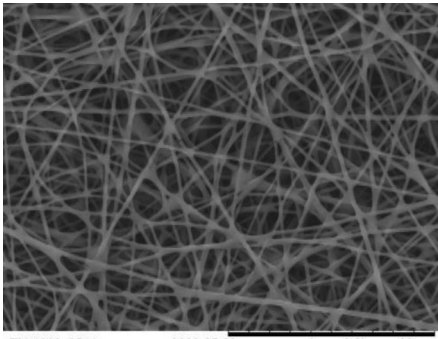
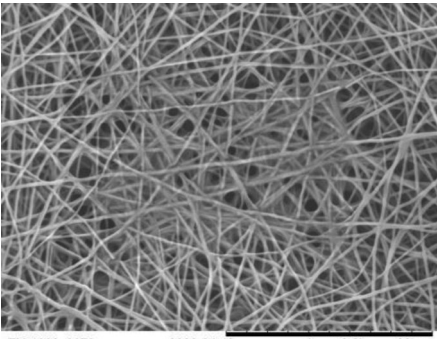


Figure 4. Mass absorbability of PBS buffer of films with different COOH:OH molar ratios.

the contribution of the material properties (autocatalysis). Reduc-

Table 2. SEM images of electrospun nonwovens made from poly-L-lactide/poly(1,3-propanediol citrate).

PLA/PDCit	COOH:OH molar ratio of poly(1,3-propanediol citrate)	
	1:1	1:2
3:1		
1:1		
1:3		

ing the influence of the latter would be possible with a cyclic exchange of the PBS buffer. The medium exchange would also simulate the circulation of body fluids under in vivo conditions. It was decided not to conduct the study this way, as the material in question was considered unprosperous. Even with frequent exchange of PBS buffer, the acidification of the medium would have been significant and disqualifying for further studies.

The other two materials degraded completely between the 60th and 90th day. The progression of weight changes during the test was similar in both cases. However, the values shown in **Figure 4** for the material with an equimolar COOH:OH ratio are certainly slightly overestimated (increase in sample weight during the test compared to the initial weight). It is due to the absorption and retention of some liquid inside the film, indicating a bulk degra-

ation mechanism. The degrading agent penetrates the material and causes hydrolysis of the ester bonds simultaneously throughout the entire volume. The varying degradation rate also confirms this. In the case of a surface degradation mechanism, the mass changes should be constant in time.

3.2. Electrospun Nonwovens

Nonwovens of PLA and poly(1,3-propanediol citrate) with a COOH:OH molar ratio of 1:2 and 1:1 were made via electrospinning. At this stage, material containing excess carboxyl groups was rejected as being too rapidly degradable in aqueous media and highly probable to be cytotoxic. The mass content of

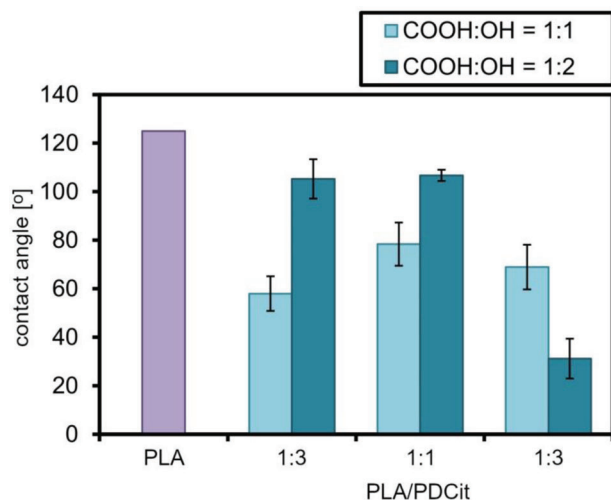


Figure 5. Water contact angle values of nonwovens with different contents of poly(1,3-propanediol citrate) and different COOH:OH molar ratios.

poly(1,3-propanediol citrate) in the polymer blend was 25% (3:1 PLA/PDCit), 50% (1:1 PLA/PDCit), and 75% (1:3 PLA/PDCit).

3.2.1. Morphology

The structure of the nonwovens was visualized using a scanning electron microscope (Table 2). It was possible to obtain a fibrous material with individual fiber diameters in the range of 0.5–5 μm. Poly-L-lactide improved processing performance. It is evident that as the mass content of PLA in the blend is reduced, the quality of the electrospun materials decreases significantly. The fibers are more poorly formed, thinner, and prone to clustering. In the case of 1:3 PLA/PDCit, a thin layer of solid material can be observed on the surface. Thus, obtaining nonwovens from pure poly(1,3-propanediol citrate) is probably impossible via electrospinning. This does not exclude using this polyester as an

additive to modify the final material's selected properties (surface, mechanical, etc.).

SEM images are insufficient to assess the nonwovens' suitability as cell culture scaffolds. However, it should be noted that the smooth surface of the fibers may result in reduced cell adhesion. All the fabrics are porous, allowing the cells to inhabit the entire volume.

3.2.2. Wettability and Surface Free Energy

A study of the contact angle between distilled water and diiodomethane on the surface of the nonwovens was carried out. It was observed that on the surface of five of the six materials, a drop of diiodomethane dissolves immediately after being applied with a syringe needle so that the contact angle value is 0°. Only in the case of 1:3 PLA/PDCit with excess hydroxyl groups (COOH:OH = 1:2) did the applied droplet remain intact for several seconds before dissolving. This allowed the determination of the diiodomethane contact angle, and the value was $(7.0 \pm 1.4)^\circ$. Hence, only the water contact angle values are shown in Figures 5 and 6.

The results are inconsistent with the hypothesis set up before the study. Adding poly(1,3-propanediol citrate) increases the hydrophilicity of the surface compared to polylactide ($\approx 125^\circ$), but the trend is unclear. It was assumed that the water contact angle should decrease with increasing poly(1,3-propanediol citrate) content. Yet, the results can be considered comparable (for COOH:OH = 1:1). Likely, the surface properties are more influenced by the arrangement of the polymer chains in the nonwovens. Polylactide forms the core of the structure, interspersed with the more hydrophilic poly(1,3-propanediol citrate). The higher surface fraction of poly(1,3-propanediol citrate) is not equivalent to its higher mass content in the electrospinning mixture. The arrangement of the polymer chains may be coincidental.

The significant increase in surface hydrophilicity of 1:3 PLA/PDCit nonwovens with an excess of hydroxyl groups (COOH:OH = 1:2) is probably due to the poor fiber-forming

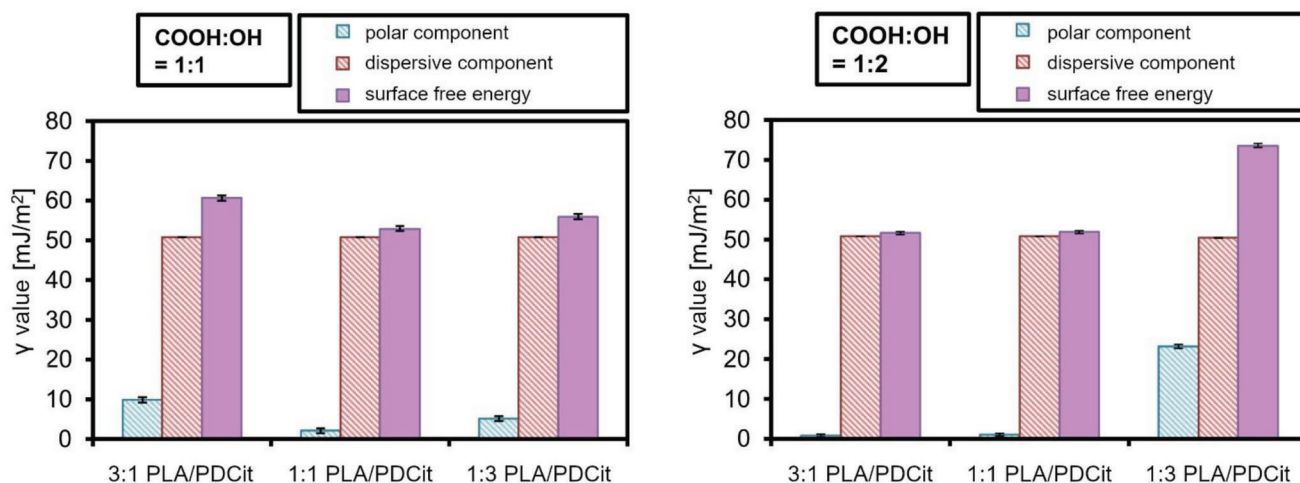


Figure 6. Surface free energy and its components of nonwovens with different contents of poly(1,3-propanediol citrate) and different COOH:OH molar ratios.

Table 3. Mechanical properties of electrospun nonwovens made from poly-L-lactide/poly(1,3-propanediol citrate); F_{\max} —maximum tensile force at break, A—elongation at break, E—Young's modulus.

PLA/PDCit	COOH:OH molar ratio of poly(1,3-propanediol citrate)					
	1:1			1:2		
	F_{\max} [N]	A [%]	E [MPa]	F_{\max} [N]	A [%]	E [MPa]
3:1	2.32	136.5 ± 5.5	13.3 ± 1.9	2.02	111.5 ± 3.5	7.5 ± 0.1
1:1	0.96	93.0 ± 4.0	3.3 ± 0.5	0.88	72.0 ± 2.0	3.1 ± 0.1
1:3	0.53	15.0 ± 0.5	1.0 ± 0.1	0.49	35.0 ± 4.0	1.0 ± 0.0

properties of this polymer. The layers of solid material observed in the SEM images are areas of increased hydrophilicity. In other cases, the PLA dominates the fiber surface, hence the high values of the water contact angle.

3.2.3. Mechanical Properties

The mechanical properties of electrospun nonwovens are determined and presented in **Table 3**.

The values of elongation at break and Young's modulus of analogous materials made only from PLA are 107% and 315 MPa, respectively.^[42] Given the acquired results, it can be concluded that a relatively small addition of PDCit (up to 25%) does not affect nonwovens elongation capability and may even improve it to some degree. Nonetheless, there is a major drop in Young's modulus, and it is explicit that the higher the concentration of PDCit, the lower the value of Young's modulus. Nonwovens with identical amounts of PDCit added to PLA are similar within the standard deviation limits if the addition is 50% or higher, differences in COOH:OH molar ratios of PDCit notwithstanding. It can be related to the comparable crosslinking degree (as seen in the gel content values of the films) for both PDCits. However, for the lowest PDCit content, the distinction in Young's modulus between those two materials is significant, yet the reason remains unclear. Sample preparation likely affects results, that is, whether they are cut perpendicularly or parallel to the nonwovens orientation. The arrangement of the nonwovens may not be homogeneous throughout the material.

Amorphous phase chain arrangement is a critical factor contributing to the mechanical response properties of the nonwovens. PLA is brittle, and the mobility of the chains is low, whereas PDCit increases molecular mobility, contributing to a reduction of Young's modulus and elongation at break. Besides, the tensile strength of the polymer increases with molecular weight. In the case of high molecular weight, polymer chains are bulky and consequently become entangled, hence the better resistance when subjected to strain. Material can be stretched further before the chains break, and more bonds must be broken, meaning the polymer can absorb more energy before rupture. PDCit added to PLA is in the form of oligomers. When the molecular weight is low, chains are loosely bound by weak intermolecular van der Waals forces. Smaller molecules have more end groups, increasing free volume and molecular mobility and consequently reducing Young's modulus.

Described influence of the poly(diols citrate) on PLA-based nonwovens contradicts the results obtained for poly(1,8-octanediol citrate) (POC).^[43] Given the significant difference in chain length between both diols, it is only reasonable for POC to exhibit much better elasticity than PDCit.

The results of this study are comparable to elastin in terms of Young's modulus for materials with higher PDCit content and strain at break for materials with higher PLA content.^[44] It implies the potential of such materials for applications in substitutes, especially of tissues characterized by high amounts of elastin, like blood vessels.

3.2.4. Thermal Properties

DSC tests were conducted to obtain the thermal properties of all PLA/PDCit(1:1) and PLA/PDCit(1:2) nonwovens, meaning 1:1 and 1:2 COOH:OH molar ratios, respectively. Both PDCit prepolymers used for electrospinning these nonwovens were also examined for comparison. Results are presented in **Figures 7–9**.

The DSC curves in Figure 7 show distinct shifts of the baseline ($T(F)$) between 100 and 220 °C, resulting from the ongoing crosslinking process of the prepolymer during the test heating. Given quite a low degree of esterification of the carboxyl groups in the PDCit(1:1) ($\approx 70\%$) and PDCit(1:2) ($\approx 79\%$) resins, heat energy uptake is significant enough to be distinguishable. Thermal decomposition of citric acid also occurs in this temperature range, leading to dehydration and decarboxylation. Also, endothermic shifts below 50 °C are observed, indicating glass transition. For the PDCit(1:1) prepolymer (green curve), glass transition temperature during the first heating ($T(A)$) is significantly lower (-10 °C) than during cooling ($T(B)$) and second heating ($T(C)$, ≈ 35 and 43 °C). This is the result of crosslinking, as mentioned above. The initial sample consists mainly of low-molecular weight oligomers with a few repeating units that form long branched chains after first heating. No melting peaks or crystallization peaks were found, as expected. The hyperbranched structure of the polymer makes it amorphous.

The same conclusions apply to the PDCit(1:2) prepolymer (blue curve). The glass transition is not visible on the first heating curve, though, probably due to negligible heat absorption, which may be caused by the prepolymer's relatively low viscosity, resulting from the excess of the alcohol. Glass transition during cooling and second heating occurs about 10 °C ($T(D)$, $T(E)$). It is a lower value than the one for PDCit(1:1) for the same reason as above.

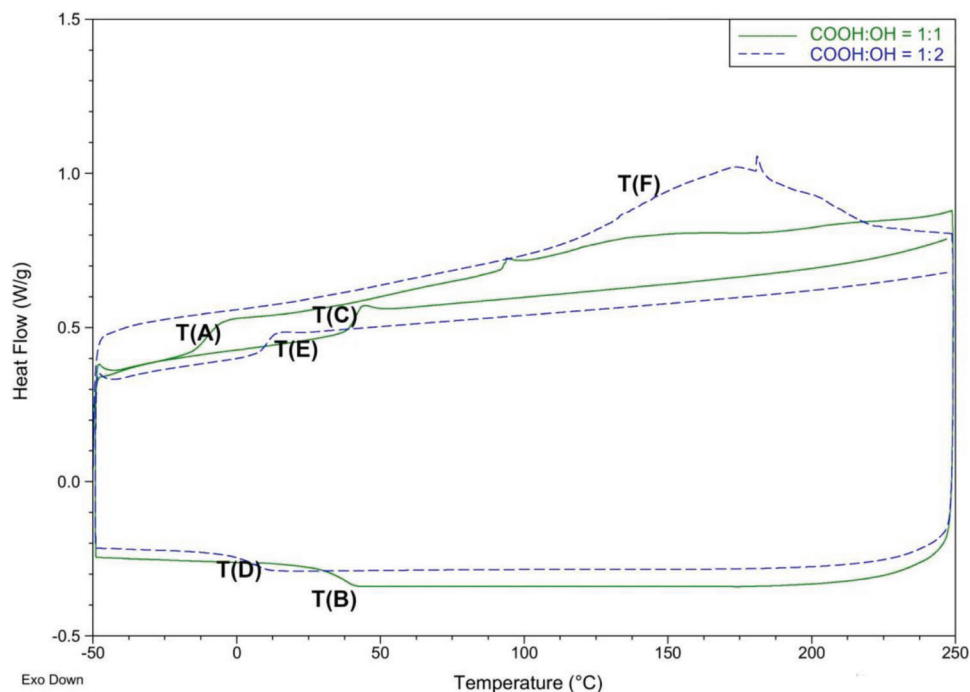


Figure 7. DSC thermogram of PDCit prepolymers with different COOH:OH molar ratios.

The DSC curves of all three nonwovens in Figure 8 indicate glass transition at about $-10\text{ }^{\circ}\text{C}$ ($T(G)$), rising to about $40\text{ }^{\circ}\text{C}$ ($T(H)$, $T(I)$) after first heating. The heat effect is less noticeable than for PDCit resin itself and increases with its mass content in the polymer blend for electrospinning. $T(J)$ at about $55\text{ }^{\circ}\text{C}$ marks

the glass transition of PLA, followed by cold crystallization, with a proportionally decreasing heat effect for lower contents of PLA (compare green and blue curves). A slight shift toward higher temperatures from 3:1 PLA/PDCit to 1:3 PLA/PDCit results from PDCit hindering crystallization by significantly increasing

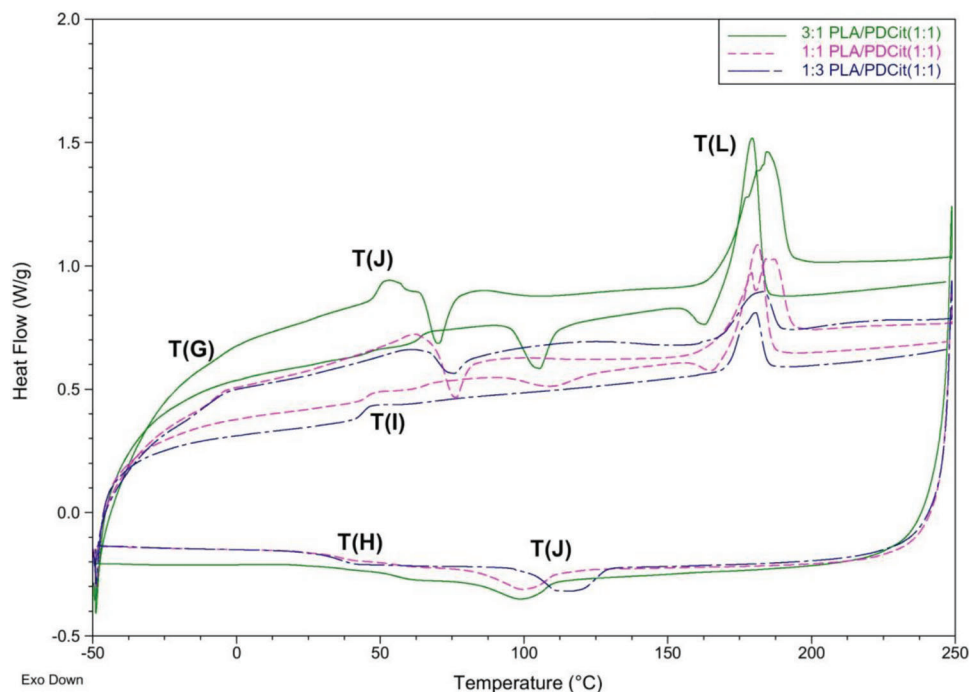


Figure 8. DSC thermogram of PLA/PDCit nonwovens with a COOH:OH molar ratio of 1:1 and with different mass contents of poly(1,3-propanediol citrate).

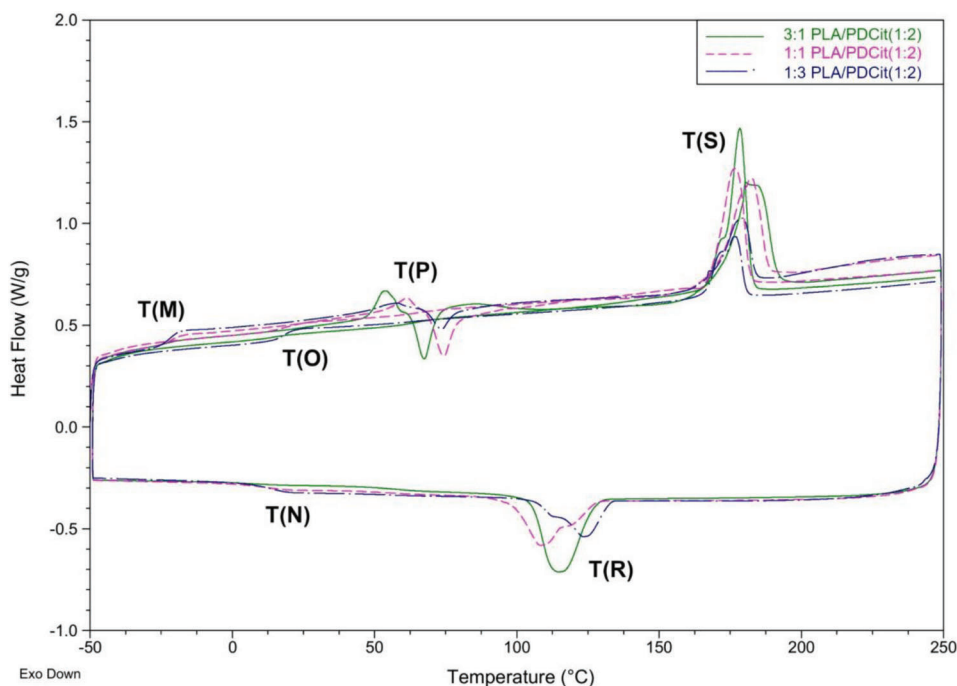


Figure 9. DSC thermogram of PLA/PDCit nonwovens with a COOH:OH molar ratio of 1:2 and with different mass contents of poly(1,3-propanediol citrate).

the content of the amorphous phase. The glass-transition-based curve shift is less sharp in the case of 1:3 PLA/PDCit compared to 3:1 PLA/PDCit due to PDCit causing the fractionation of PLA chains differing in length. Between $T(K)$ and $T(L)$ points PDCit prepolymer crosslinking can be observed, most distinctive on the blue curve. At around 175 °C ($T(L)$), melting of PLA can be noticed, probably overlapping with dehydration and decarboxylation of citric acid-based parts. Interestingly, during the first heating, the PLA-melting signal shows two distinguishable peaks, probably coming from fractions with different chain lengths. The effect is diminished by the time of the second heating due to various possible effects: partial degradation of PDCit (lesser impact on fractionation), PLA reacting with PDCit (via free terminal carboxyl groups in PLA and OH groups in PDCit), or homogenization of PLA chain lengths because of different fractions reacting with each other.

The effects observed for PLA/PDCit(1:2) nonwovens (Figure 9) are comparable to the above, with the glass transition temperatures of the polycitrate parts being accordingly lower than for PDCit(1:1), as already described regarding Figure 7 (compare $T(D)$ and $T(E)$ with $T(N)$ and $T(O)$). Note that there is a detectable glass transition during the first heating for the nonwoven with the highest PDCit content ($T(M)$) at about -20 °C. Considering relatively small differences for the respective curves between the three types of nonwovens, it can be presumed that the effect of PDCit(1:2) on the properties of the whole nonwoven is much weaker than for PDCit(1:1), which may be related to the difference in viscosity of the two prepolymers. PDCit(1:2), being less viscous, is more easily mixed in PLA.

Given the good performance of typical citric acid triesters, it is possible to expect the plasticizer-like effect of low-molecular

weight PDCit. However, its content in those nonwovens is too high to observe any actual effect of this kind.

Based on DSC analysis, the degree of crystallinity of the nonwovens was determined (Figure 10).

It was observed that the degree of crystallinity of nonwovens decreases with increasing PDCit content because of the hyper-branched structure of citrate polyester. This decrease is less noticeable with PDCit(1:2), possibly due to the lower molecular weight and lower degree of branching associated with the lower citric acid content. Such a structure makes the crystallization of

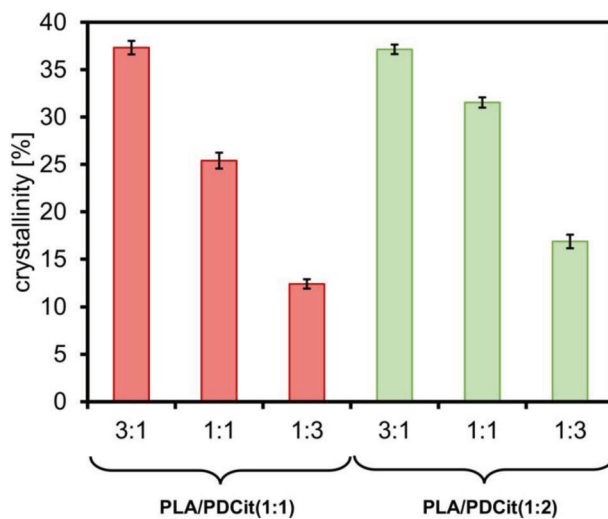


Figure 10. Degree of crystallinity of nonwovens with different contents of poly(1,3-propanediol citrate) and different COOH:OH molar ratios.

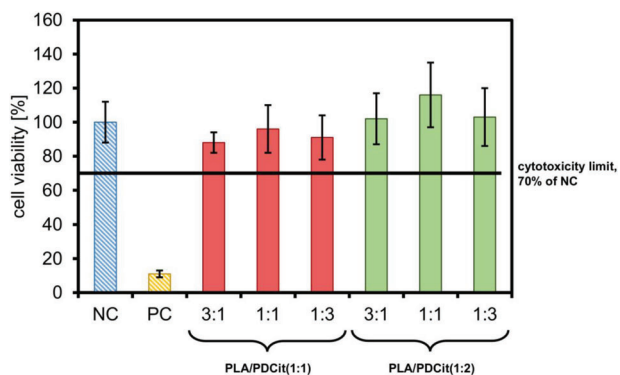


Figure 11. Cytotoxic effect of the 24 h extracts of the various PLA/PDCit nonwovens as a percentage of the negative control (NC) viability. The black line shows the accepted cytotoxicity limit at 70% of NC. Positive control (PC) is the result of the activity of the cells cultured with TritonX-100.

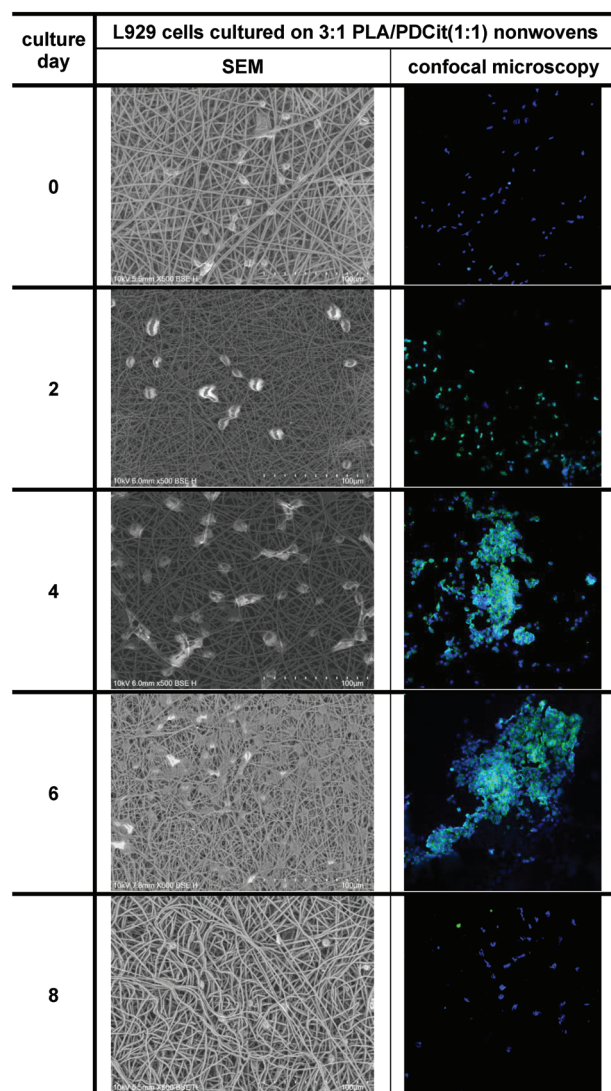


Figure 12. Morphology assessment of L929 cells using SEM (left) and confocal microscopy (right). Culture on 3:1 PLA/PDCit(1:1) nonwovens.

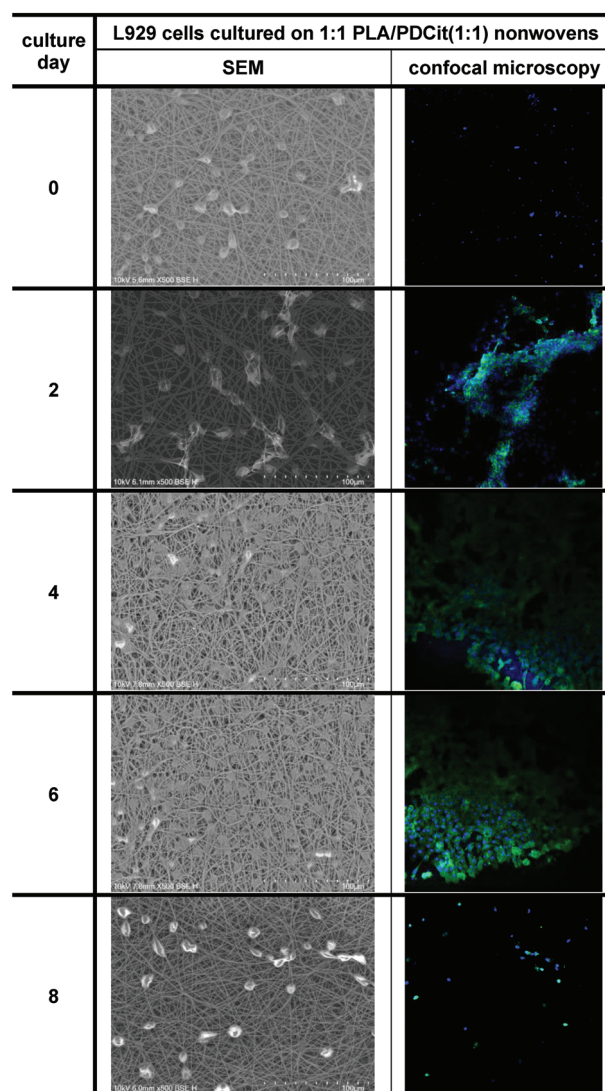


Figure 13. Morphology assessment of L929 cells using SEM (left) and confocal microscopy (right). Culture on 1:1 PLA/PDCit(1:1) nonwovens.

linear PLA less hindered, and the short oligomeric chains of the polycitrate are more easily intermixed with the base polymer.

4. L929 Cell-Based Assays of PLA/PDCit Nonwovens

4.1. Cytotoxicity Tests

The cytotoxicity effect of the PLA/PDCit nonwovens was investigated by the results of the colorimetric XTT reagent assay. L929 mouse fibroblasts were used. Cell viability determination was based on the absorbance measured spectrophotometrically at 450 and 660 nm in the XTT test, following ISO EN 10993-5: 2009. Initially, the intention was to perform cytotoxicity tests on films additionally, but this idea was abandoned due to the culture medium acidifying too quickly. Results of the XTT cytotoxicity tests of the nonwovens are presented in **Figure 11**.

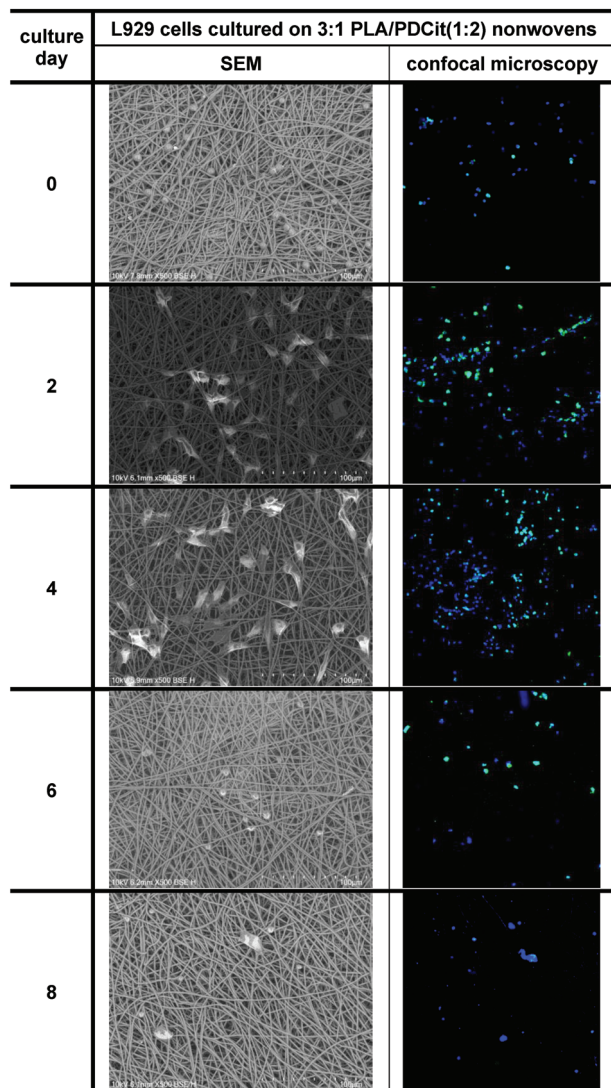


Figure 14. Morphology assessment of L929 cells using SEM (left) and confocal microscopy (right). Culture on 3:1 PLA/PDCit(1:2) nonwovens.

None of the tested nonwovens exhibits a short-term cytotoxic effect on L929 cells as the metabolic activity does not drop below 70% of negative control, commonly set as the cytotoxicity limit. The obtained results do not indicate an increase in cytotoxicity even at higher contents of poly(1,3-propanediol citrate) (1:3 type nonwovens), which in theory, should acidify the culture medium most rapidly. It is likely that the presence of semicrystalline PLA limits the penetration of the medium into the material and inhibits degradation.

4.2. Eight Days Cell Culture

L929 cells were maintained for 8 days, with samples harvested every 48 h. Images of cells after staining are presented in **Figures 12–15** alongside SEM images of cells on nonwovens. The actin skeleton of the cells is stained green, and the nuclei are stained blue. **Figures 16** and **17** present changes in different cul-

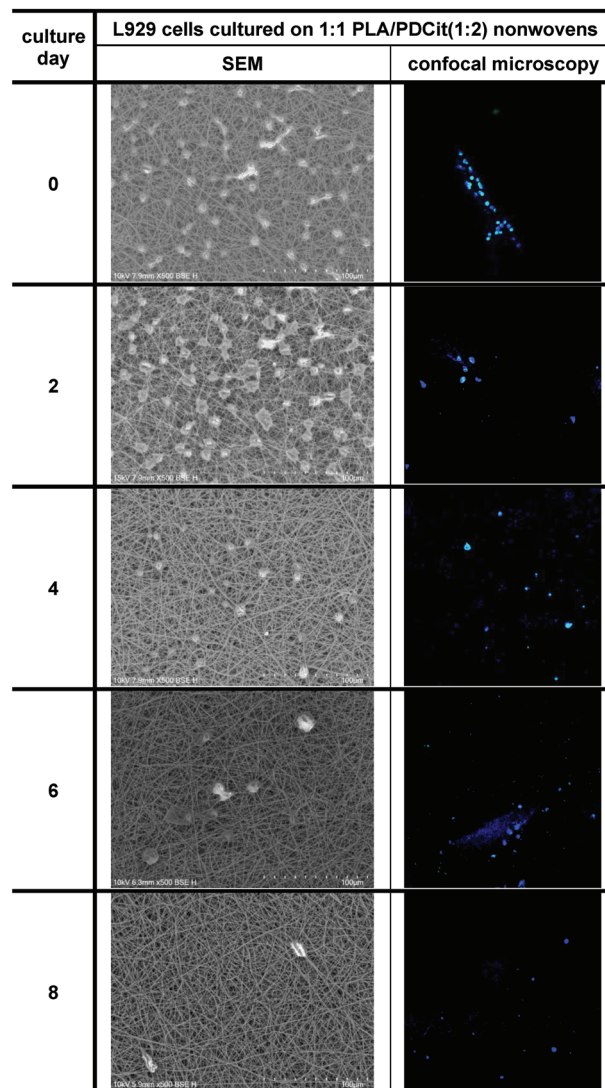


Figure 15. Morphology assessment of L929 cells using SEM (left) and confocal microscopy (right). Culture on 1:1 PLA/PDCit(1:2) nonwovens.

ture parameters for all the materials compared to the reference culture.

The overall morphology of the cells cultured on the nonwovens differs from those growing on the flat reference surface.^[45–47] It is to be expected given the nonwovens' fibrous and highly porous structure. To adhere to such a surface, the cells often must wrap themselves around the fibers and take on a more elongated shape due to the limited number of attachment sites. Not until later in the culture time (>4 days), when the cells start to form a dense colony, do they adopt more of a cobblestone-like shape.

For both types of the PLA/PDCit(1:1) nonwovens, it is apparent that while the number of cells increases up to the sixth day of culture, on the eighth day the growth is suppressed (**Figure 16A–F**). Cell viability decreased due to nutrient consumption in the medium, increased concentration of metabolic waste, and reduced available growth area. This effect is comparable to the reference culture and, as such, should not be associated with the

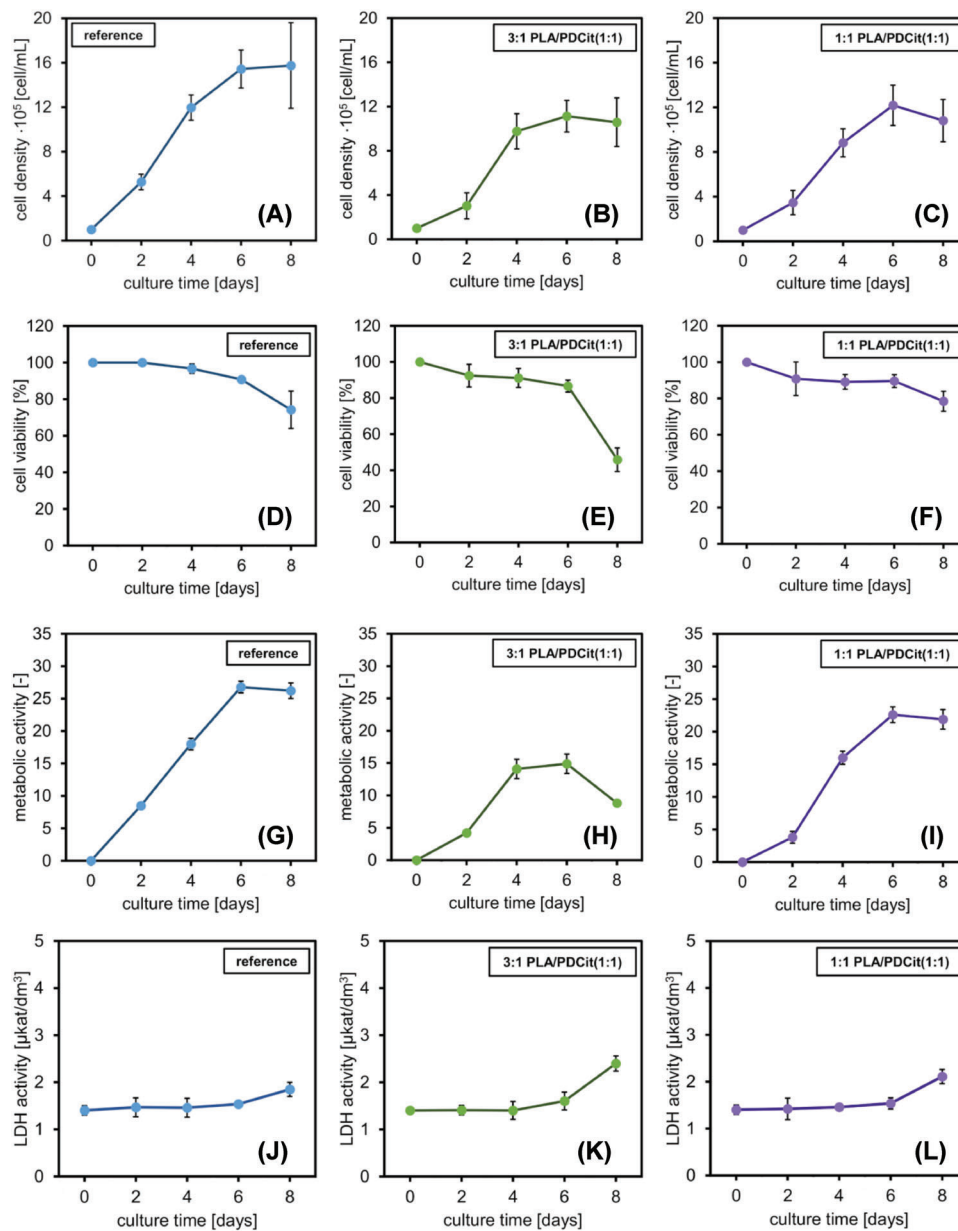


Figure 16. a–l) L929 culture properties at different time points: cell density, cell viability, metabolic activity, and LDH activity. Comparison between the reference culture and the PLA/PDCit nonwovens of an equimolar COOH:OH ratio with a different mass content of poly(1,3-propanediol citrate): 25% (3:1 PLA/PDCit(1:1)) and 50% (1:1 PLA/PDCit(1:1)).

potential cytotoxicity of the nonwovens. Due to their low density, the nonwovens partially floated in the culture medium, reducing the number of adhered cells. Not all cells managed to settle on the material and floated down the porous structure. This effect is noticeable in the slower growth of cells between days 0 and 2 compared to the reference. The growth rate from the second to fourth day and from the fourth to sixth day parallels the reference culture, indicating that the adhered cells are growing on the nonwovens. A more substantial decrease in cell viability between days 0 and second compared to days second and sixth may be specifically due to the non-adherence of some cells from the suspension applied on the nonwovens (compare Figure 16E–F

with Figure 16D). This hypothesis is supported by confocal microscopy and SEM images, showing the increasing number of cells over time.

The circumstances are different for the PLA/PDCit(1:2) nonwovens. There is hardly any cell growth detected on 1:1 PLA/PDCit(1:2) material, as seen in Figure 17C/F/I/L and provided SEM and confocal images. There is a slight increase in the number of cells after 2 days of culture, followed presumably by acidification of the local environment. This effect was not detected during the cytotoxicity testing and is also not entirely confirmed here, as no drop in the pH of the culture medium has been observed. However, it is possible that no intensive acidification

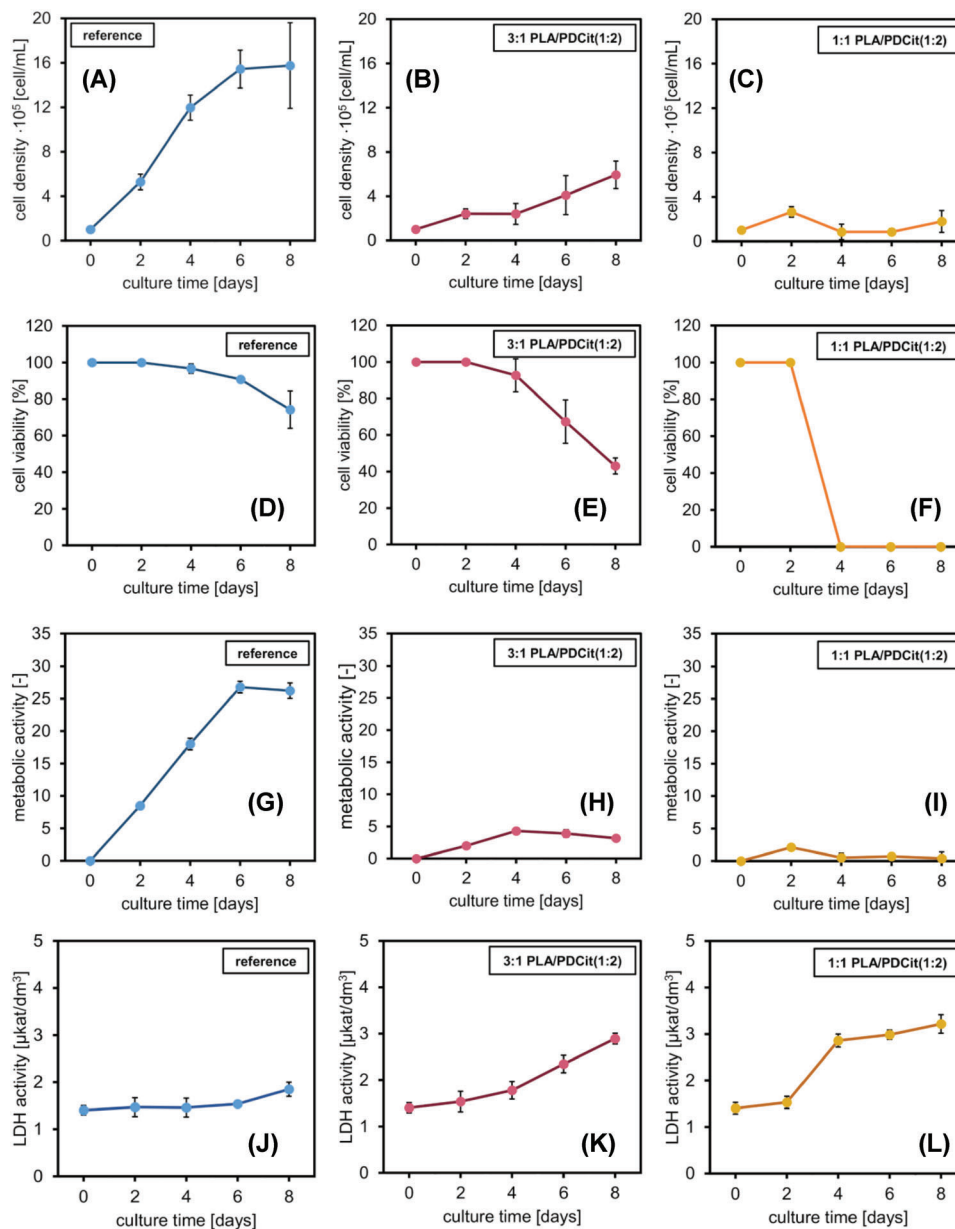


Figure 17. a–l) L929 culture properties at different time points: cell density, cell viability, metabolic activity, and LDH activity. Comparison between the reference culture and the PLA/PDCit nonwovens of 1:2 COOH:OH molar ratio with a different mass content of poly(1,3-propanediol citrate): 25% (3:1 PLA/PDCit(1:2)) and 50% (1:1 PLA/PDCit(1:2)).

of the medium is occurring because the material's degradation is not advancing substantially. Still, poly(1,3-propanediol citrate) with excess hydroxyl groups exhibits a somewhat higher degradation rate than the equimolar one due to the lower crosslinking density (as discussed in the previous sections of the article). For this reason, cells in direct contact with the fibers of a nonwoven can sense and respond to these slight changes. The same explanation can be applied to material 3:1 PLA/PDCit(1:2), but this effect is less prominent given the lower PDCit content. Nonetheless, cell growth at the beginning (zeroth to second day) is slower compared to the reference, indicating a longer adaptation time (compare Figure 17A with Figure 17B). Once adapted to the con-

ditions, the cells start to grow on the material, but the growth is quite stunted.

Figures 16j–l and 17j–l show the LDH activity. LDH release assay was used to assess the level of plasma membrane damage in cell culture: the higher the enzyme concentration, the more recently damaged cells. The results are complementary to the cell density and viability assessment. The most significant increase of LDH activity in the reference culture occurs after 6 days, indicating hindered proliferation of cells despite the highest values of metabolic activity. It confirms the conclusions regarding cell death prompted by high confluency and their competition for space on the plate surface, enhanced by the depletion of the

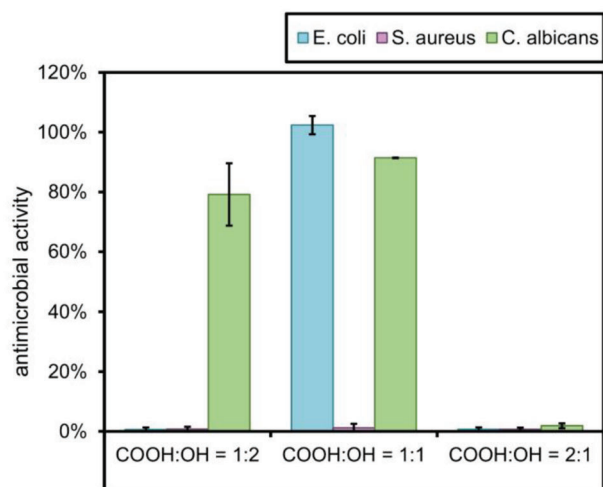


Figure 18. Antimicrobial activity of poly(1,3-propanediol citrate) films with different COOH:OH molar ratios as a percentage of culture growth inhibition.

culture media. As seen in Figure 16K,L, the same conclusions can be made about both types of the PLA/PDCit(1:1) nonwovens, except the increase in LDH activity between days sixth and eighth is more pronounced. The higher cell damage rate may be due to a smaller specific surface area of growth (porosity, fibrous rather than solid structure) and, therefore, a faster critical confluence value being reached. Remarkably, both metabolic activity and LDH activity profiles are, in this case, much more similar to the reference for nonwovens with a higher PDCit content (1:1 PLA/PDCit(1:1), Figure 16I,L). It may indicate the positive effect of the addition of a polymer that hydrophilizes the PLA surface while not acidifying the cell environment (slow degradation rate).

For materials PLA/PDCit(1:2), the results obtained for metabolic activity and LDH activity (Figure 17J–L) confirm significant cell death occurring already from the beginning, which is in line with previous remarks about the acidity of the surface of the nonwovens. Cell damage and death are more rapid for higher mass content of PDCit(1:2), happening extensively as early as second day of culture.

5. Antimicrobial Activity of the Polymer Films

5.1. Tests in the Liquid Medium

The antimicrobial activity of poly(1,3-propanediol citrate) films with different COOH:OH molar ratios has been tested in the liquid medium. The inhibitory effect of the materials was determined by a decrease in OD compared to the control culture (Figure 18). After the incubation with polymer films, the pH values of the culture medium were measured (Table 4). Samples were not weighed after removal from the medium. Still, the majority of them (COOH:OH = 1:1 and 1:2) retained their original shape and size, from which it can be assumed that no extensive degradation occurred. Films with an excess of carboxyl groups degraded completely.

It is apparent that the antimicrobial activity of PDCit films results from the pH drop in the culture medium. The growth of

Table 4. PH of culture medium after 24 h incubation with polymer films.

	COOH:OH molar ratio of poly(1,3-propanediol citrate)		
	1:2	1:1	2:1
<i>E. coli</i>	4.5	6.5	3.0
<i>S. aureus</i>	4.5	6.5	3.0
<i>C. albicans</i>	3.5	5.0	2.0

Table 5. Antimicrobial activity of poly(1,3-propanediol citrate) films with different COOH:OH molar ratios as the diameter of inhibition growth zone [mm].

	COOH:OH molar ratio of poly(1,3-propanediol citrate)		
	1:2	1:1	2:1
<i>E. coli</i>	0	0	29.4 ± 2.2
<i>S. aureus</i>	0	0	30.9 ± 2.0
<i>C. albicans</i>	0	0	23.0 ± 1.9

C. albicans, the most resistant to the acidic environment among the three tested microorganisms, is significantly inhibited only after contact with the material with excess carboxyl groups (lowest pH). Differences in pH changes between the materials are comparable to the results obtained during degradation testing, with the equimolar COOH:OH ratio film being the least acidifying, which is the consequence of the highest content of the crosslinked polymer. The slightly sharper decrease in pH for *C. albicans* is a result of the metabolic activity of this yeast.

5.2. Tests on the Solid Medium

The antimicrobial activity of the PDCit films was additionally determined by the size of the inhibition of the growth zone. The results are partially comparable to the tests conducted in the liquid medium (Table 5 and Figure 19). Only the material with excess carboxyl groups exhibits antimicrobial activity against all tested microorganisms resulting from media acidification. The apparent difference in pH decrease compared to the liquid medium is presumably a consequence of the diffusion rate. Given enough time, all the film samples would sufficiently degrade and induce microbial growth inhibition.

Initially adherent to the media surface, the discs cut from the most acidic PDCit have become mostly detached and rolled up (as seen in Figure 19).

6. Conclusions

In this work a polyester was prepared from citric acid and 1,3-propanediol. Films of poly(1,3-propanediol citrates) with different stoichiometry of COOH:OH groups were made. The wettability of the film surfaces was investigated with a polar (water) and a non-polar liquid (diiodomethane). The surface free energy of the materials was calculated. It was observed that the films showed wettability with both liquids, with an excess of hydroxyl groups in the material increasing the hydrophilicity of its surface.

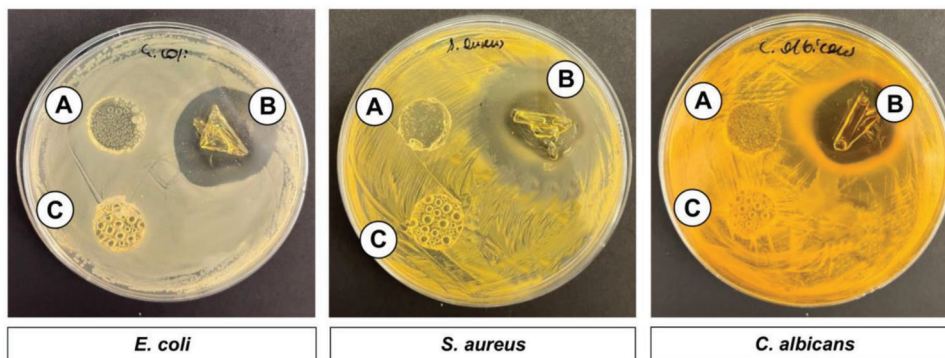


Figure 19. Antimicrobial activity of poly(1,3-propanediol citrate) films with different COOH:OH molar ratios: A: 1:1, B: 2:1, C: 1:2, tested on a solid medium.

Poly(1,3-propanediol citrate) films have been shown to be capable of absorbing and retaining polar liquid in their structure. This may enable the material to be saturated with bioactive liquids.

The stoichiometry of the functional groups strongly influenced the course of the films degradation. Materials with an equal content of functional groups or an excess of hydroxyl groups are completely degraded after more than 60 days. Degradation occurs via bulk mechanism.

Nonwovens were prepared by electrospinning from a mixture of poly(1,3-propanediol citrates) and PLA. It was found that poly(1,3-propanediol citrate) exhibited low fiber-forming potential on its own, but could be used together with another polymer as an additive to hydrophilize the surface and promote cell adhesion. The materials exhibited potential as antimicrobial agents, primarily due to the acidification of the culture environment. In the case of PLA/PDCit nonwovens, the amount of polycitrate may be too small to produce a similar effect. However, these are preliminary results that suggest the possibility of using the polymer as an antimicrobial agent, not necessarily strictly as presented. The polymer could, for example, serve as an antibacterial additive in cosmetic formulations or be released from another carrier in a controlled manner.

Acknowledgements

This scientific research was financed from the budgetary funds of The Excellence Initiative—Research University Programme (BIOTECHMED-3 Advanced)—“Biomimetic, biodegradable cell scaffolds for the differentiation of stem cells into osteoblasts and chondrocytes (SteamScaf).” The authors would like to thank Faculty of Chemistry, Warsaw University of Technology for providing the laboratory equipment.

Conflict of Interest

The authors declare no conflict of interest.

Data Availability Statement

The data that support the findings of this study are available from the corresponding author upon reasonable request.

Keywords

biomaterials, cell cultures, citric acid polyesters, electrospinning, poly(1,3-propanediol citrate), polymer films

Received: July 27, 2023
Revised: October 10, 2023
Published online: October 25, 2023

- [1] F. Zhang, M. W. King, *Adv. Healthcare Mater.* **2020**, *9*, 1901358.
- [2] O. Janousková, *Physiol. Res.* **2018**, *67*, S335.
- [3] M. J. Austin, A. M. Rosales, *Biomater. Sci.* **2019**, *7*, 490.
- [4] A. Muñoz-Bonilla, C. Echeverría, Á. Sonseca, M. P. Arrieta, M. Fernández-García, *Materials* **2019**, *12*, 641.
- [5] L. Gritsch, C. Lovell, W. H. Goldmann, A. R. Boccaccini, *J. Mater. Sci. Mater. Med.* **2018**, *29*, 18.
- [6] Q. Jin, M. F. Kirk, *Front. Environ. Sci.* **2018**, *6*, 21.
- [7] R. Sánchez-Clemente, M. I. Igeño, A. G. Población, M. I. Guijo, F. Merchán, R. Blasco, *Proceedings* **2018**, *2*, 1297.
- [8] O. R. Kotsyurbenko, K.-J. Chin, M. V. Glagolev, S. Stubner, M. V. Simankova, A. N. Nozhevnikova, R. Conrad, *Environ. Microbiol.* **2004**, *6*, 1159.
- [9] D. Fernández-Calviño, E. Bääth, *FEMS Microbiol. Ecol.* **2010**, *73*, 149.
- [10] A. R. Amini, J. S. Wallace, S. P. Nukavarapu, *J. Long Term Eff. Med. Implants* **2011**, *21*, 93.
- [11] P. Jariyasakoolroj, P. Leelaphiwat, N. Harnkarnsujarit, *J. Sci. Food Agric.* **2020**, *100*, 5032.
- [12] C. Moya-Lopez, J. González-Fuentes, I. Bravo, D. Chapron, P. Bourson, C. Alonso-Moreno, D. Hermida-Merino, *Pharmaceutics* **2022**, *14*, 1673.
- [13] F. Qi, M. Tang, X. Chen, M. Chen, G. Guo, Z. Zhang, Z. Zhang, *Eur. Polym. J.* **2015**, *71*, 314.
- [14] S. Marano, E. Laudadio, C. Minnelli, P. Stipa, *Polymers* **2022**, *14*, 1626.
- [15] T. Liu, R. Huang, X. Qi, P. Dong, Q. Fu, *Polymer* **2017**, *114*, 28.
- [16] Q. Ou-Yang, B. Guo, J. Xu, *ACS Omega* **2018**, *3*, 14309.
- [17] V. Sivanjineyulu, K. Behera, Y.-H. Chang, F.-C. Chiu, *Compos. Part A Appl. Sci. Manuf.* **2018**, *114*, 30.
- [18] W. Phetwarotai, N. Phusunti, D. Aht-Ong, *Chin. J. Polym. Sci.* **2019**, *37*, 68.
- [19] A. Kowalewska, M. Nowacka, *Molecules* **2020**, *25*, 3351.
- [20] D. Zhao, T. Zhu, J. Li, L. Cui, Z. Zhang, X. Zhuang, J. Ding, *PolyBioact. Mater.* **2021**, *6*, 346.
- [21] P. Piszko, B. Kryszak, A. Piszko, K. Szustakiewicz, *Polim. Med.* **2021**, *51*, 43.
- [22] Z. Li, J. Yang, X. J. Loh, *NPG Asia Mater.* **2016**, *8*, e265.
- [23] I. Navarro-Baena, V. Sessini, F. Dominici, L. Torre, J. M. Kenny, L. Peponi, *Polym. Degrad. Stab.* **2016**, *132*, 97.
- [24] Y. Zhong, P. Godwin, Y. Jin, H. Xiao, *Adv. Ind. Eng. Polym. Res.* **2020**, *3*, 27.
- [25] J.-W. Rhim, S.-I. Hong, C.-S. Ha, *LWT* **2009**, *42*, 612.

- [26] E. Mascheroni, V. Guillard, F. Nalin, L. Mora, L. Piergiovanni, *J. Food Eng.* **2010**, *98*, 294.
- [27] C. Villegas, A. Torres, M. Rios, A. Rojas, J. Romero, C. L. De Dicastillo, X. Valenzuela, M. J. Galotto, A. Guarda, *Food Res. Int.* **2017**, *99*, 650.
- [28] Y. Liu, S. Wang, R. Zhang, W. Lan, W. Qin, *Nanomaterials* **2017**, *7*, 194.
- [29] T. Min, X. Sun, Z. Yuan, L. Zhou, X. Jiao, J. Zha, Z. Zhu, Y. Wen, *LWT* **2021**, *135*, 110034.
- [30] A. Rojas, E. Velásquez, C. P. Vidal, A. Guarda, M. J. Galotto, C. L. de Dicastillo, *Antioxidants* **2021**, *10*, 1976.
- [31] M. Bautista, A. Martínez De Ilarduya, A. Alla, M. Vives, J. Morató, S. Muñoz-Guerra, *Eur. Polym. J.* **2016**, *75*, 329.
- [32] D. M. Panaitescu, E. R. Ionita, C.-A. Nicolae, A. R. Gabor, M. D. Ionita, R. Trusca, B.-E. Lixandru, I. Codita, G. Dinescu, *Polymers* **2018**, *10*, 1249.
- [33] X. Tang, J. Dai, H. Sun, S. Nabanita, S. Petr, L. Tang, Q. Cheng, D. Wang, J. Wei, *J. Nanomater.* **2018**, <https://doi.org/10.1155/2018/5470814>.
- [34] C. Burel, A. Kala, L. Purevdorj-Gage, *Lett. Appl. Microbiol.* **2021**, *72*, 332.
- [35] L. Zhu, Y. Zhang, Y. Ji, *J. Mater. Sci. Mater. Med.* **2017**, *28*, 93.
- [36] S. Pourshahrestani, E. Zeimaran, N. A. Kadri, N. Gargiulo, H. M. Jindal, K. Hasikin, S. V. Naveen, S. D. Sekaran, T. Kamarul, *Mater. Sci. Eng., C* **2019**, *98*, 1022.
- [37] D. Kolbuk, O. Jeznach, M. Wrzecieonek, A. Gadomska-Gajadhur, *Polymers* **2020**, *12*, 1731.
- [38] M. Wrzecieonek, A. Bandzerewicz, E. Dutkowska, J. Dulnik, P. Denis, A. Gadomska-Gajadhur, *Polym. Adv. Technol.* **2021**, *32*, 3955.
- [39] R. Z. Khoo, H. Ismail, W. S. Chow, *Procedia. Chem.* **2016**, *19*, 788.
- [40] Á. Conejero-García, H. R. Gimeno, Y. M. Sáez, G. Vilariño-Feltre, I. Ortuño-Lizarán, A. Vallés-Lluch, *Eur. Polym. J.* **2017**, *87*, 406.
- [41] A. Bandzerewicz, A. Gadomska-Gajadhur, *Cells* **2022**, *11*, 914.
- [42] D. Kolbuk, O. Jeznach, M. Wrzecieonek, A. Gadomska-Gajadhur, *Polymers* **2020**, *12*, 1731.
- [43] F. Zou, X. Sun, X. Wang, *Polym. Degrad. Stab.* **2019**, *166*, 163.
- [44] D. B. Camasão, D. Mantovani, *Mater. Today Bio.* **2021**, *10*, 100106.
- [45] K. Ulatowski, K. Wierzchowski, J. Fiuk, P. Sobieszuk, *Langmuir* **2022**, *38*, 8575.
- [46] V. Cannella, R. Altomare, G. Chiaramonte, S. Di Bella, F. Mira, L. Russotto, P. Pisano, A. Guercio, *Biomed. Res. Int.* **2019**, <https://doi.org/10.1155/2019/3469525>.
- [47] J. Jagiello, M. Kusmierz, E. Kijenska-Gawronska, M. Winkowska-Struzik, W. Swieszkowski, L. Lipinska, *Mater. Today Commun.* **2021**, *26*, 102056.